From Figs. 1 and 2 we see that there is a good overlap of Tl^+ emission resulting from the $^3P_1$-$^1S_0$ transition[5] with the $^6P_{7/2}$ state of gadolinium. The population of the $^3P_1$ level is fed from the $^3P_0$ metastable level which acts as a trap and causes a delayed fluorescence with a time constant of about 400 nsec.[6] Therefore, the time of finding electrons in the $^3P_1$ level is long enough to permit energy transfer from that level to a resonant $^6P_{7/2}$ level of gadolinium. This finding will permit the increase of gadolinium fluorescence on excitation at 253 nm.

*Work partially supported by the National Bureau of Standards under Contract No. G-103.

[1]E. Nakazawa and S. Shinoya, J. Chem. Phys. 47, 3211 (1967).
[2]R. Reisfeld, E. Greenberg, R. Velapoldi, and B. Barnett, J. Chem. Phys. 56, 1968 (1972).
[3]R. Reisfeld and L. Boehm, Solid State Chem. 4, 417 (1972).
[4]R. Reisfeld and Y. Eckstein, Solid State Chem. (to be published).
[5]Renata Reisfeld, National Bureau of Standards Conference on Accuracy in Spectrophotometry and Luminescence Measurements, Gaithersburg, Md., 1972 (unpublished).
[6]R. Reisfeld, E. Greenberg, T. Deinum, C.J. Werkhoven, and J.D.W. van Voorst (unpublished).

Enhancement of self-focusing threshold in sapphire with elliptical beams*

C.R. Giuliano
Hughes Research Laboratories, Malibu, California 90265
J.H. Marburger
University of Southern California, Los Angeles, California 90007
A. Yariv
California Institute of Technology, Pasadena, California 91101
(Received 30 March 1972)

The power threshold for optically induced bulk damage in sapphire is a sensitive function of the ellipticity of the incident beam shape. Experimental results are consistent with a simple self-focusing theory.

We wish to report observations of the strong influence of departures from circularity of an optical beam on the power threshold for optically induced bulk damage in sapphire. This threshold, which is known to arise from the formation of a catastrophic self-focus in the medium,[1] is found to increase appreciably when the beam cross section is distorted from a circle to an ellipse, and when vertical and horizontal confocal parameters differ (leading to ellipsoidal phase fronts). These observations are consistent with the theoretical predictions of Vorob'yev[2] and Shvartsburg,[3] which are extended slightly here to apply to our experiment.

Our experiments were performed using the output of a single-mode Q-switched ruby laser and amplifier focused inside sapphire samples with different lenses. The laser and associated monitoring apparatus are described in detail elsewhere.[4] The far-field beam profile was measured to be Gaussian down to 8% of the peak, using a modified multiple-lens camera technique. Typical pulse lengths are 20 nsec. The sapphire samples are typically 3-in.-long by $\frac{1}{4}$-in.-square bars.

Damage threshold powers for circular beams of different sizes are shown in Table I and compared with results for elliptical beams. The first three entries in Table I show the increased threshold power with beam size indicating the influence of electrostriction.[1] The dimensions listed in Table I are those at the beam waist, near which the self-focus first forms at threshold for circular beams. The remaining entries in Table I show the effect of noncircular beam shapes. The fourth entry gives the threshold power for an elliptical beam whose short dimension is the same as the first entry, whose long dimension is the same as the third entry, and whose area is the same as the second entry. We see that the threshold power is appreciably higher for the elliptical beam compared with any of the circular beams. The last two entries in Table I show data for more elongated elliptical beams where we were unable to reach threshold at the maximum power available from our system.

Each power threshold in Table I was determined from a series of eight laser shots of differing peak powers. When damage occurred, the damaged region was found to possess a circular rather than an elliptical cross section. In fact, the appearance of the damage tracks formed above threshold was indistinguishable from those caused by circular beams. The tracks themselves were confined to the region between the two line foci of our astigmatic optical system, but there is no evidence that they would not extend beyond the upstream focus at higher powers.

To correlate these observations with theory, we have found it necessary to resort to the "paraxial-ray–constant-shape" analysis of self-focusing outlined in Ref. 5. More accurate numerical solutions of the nonlinear wave equation, such as those employed in Ref. 1, are extremely difficult to obtain in this case, because the noncircular beam shape requires an additional degree of freedom in the computer code. Nevertheless, the approximate analysis has had some qualitative success,[6] and leads to simple expressions.

TABLE I. Comparison of damage threshold powers for circular and elliptical beams of different sizes.

Type of beam	Radius[a] (μm)	Area (μm^2)	Damage threshold power (MW)	Astigmatic focal length[b] in medium (cm)
Circular beams	14	6.3×10^2	0.51 ± 0.04	•••
(dimensions at low-	37	44×10^2	0.74 ± 0.07	•••
intensity waist)	100	308×10^2	1.23 ± 0.10	•••
Elliptical beams (dimen-	14×100	44×10^2	6.0 ± 0.50	2.99
sions at upstream low-	14×1200	535×10^2	>17[c]	∞
intensity waist)	7×1200	270×10^2	>17[c]	∞

[a]The beam radius is defined as the $1/e$ radius for the intensity.
[b]This is the distance between the two line foci [see M. Born and E. Wolf, *Principles of Optics*, 3rd Ed. (Pergamon, London, 1965), p. 171].
[c]Unable to reach threshold at this power.

Assuming an optical field of the form

$$E=\tfrac{1}{2}E_0\exp(i\varphi)\exp[i(kz-\omega t)]+\text{c.c.},$$
$$E_0=E_m(z)\exp[-\tfrac{1}{2}(x^2/a^2+y^2/b^2)],$$

we find by the method of Ref. 5 the following equations for the horizontal and vertical beam parameters a and b:

$$k^2\frac{d^2a}{dz^2}=\frac{1}{a^3}-\frac{\eta}{a^2b}, \tag{1}$$

$$k^2\frac{d^2b}{dz^2}=\frac{1}{b^3}-\frac{\eta}{ab^2}. \tag{2}$$

Here $\eta=P/P_1$, where P is the total power and $P_1=n^3c/4\epsilon_2k^2$ in Gaussian units. The first terms on the right-hand sides of Eqs. (1) and (2) represent the effect of diffraction, while the second terms arise from the nonlinear contribution $\frac{1}{2}\epsilon_2E_0^2$ to the dielectric constant. n is the linear refractive index. Vorob'yev,[2] who derived Eqs. (1) and (2) in a different way, has shown that they imply

$$\frac{d^3}{dz^3}(a^2+b^2)=0, \tag{3}$$

which can be integrated to give

$$k^2(a^2+b^2)=[k^2(\dot a_0^2+\dot b_0^2)+(2/a_0b_0)(\eta_c-\eta)]z^2+2k^2(a_0\dot a_0+b_0\dot b_0)z+k^2(a_0^2+b_0^2). \tag{4}$$

Here a_0 and b_0 are the axes of the ellipse formed by the e^{-1} points of the transverse intensity profile at $z=0$, and $\eta_c=a_0/2b_0+b_0/2a_0$. The initial rates of change $\dot a_0$ and $\dot b_0$ are simply related to the principal radii of curvature R_a and R_b of the phase fronts at $z=0$:

$$R_a=a_0/\dot a_0,\quad R_b=b_0/\dot b_0.$$

Using Eq. (4), the reader may easily find that the on-axis intensity, which is inversely proportional to $2ab\le a^2+b^2$, becomes infinite at the point

$$z_{f\infty}=ka_0b_0(\eta/\eta_c-1)^{-1/2}, \tag{5}$$

for plane incident phase fronts and $\eta>\eta_c$. It is therefore clear that the critical power for self-focusing is

$$P_c=\eta_cP_1\quad(R_a=R_b=\infty), \tag{6}$$

which equals P_1 for circular beams. For finite values of R_a and R_b, a real solution for z of the condition $a^2+b^2=0$ occurs only if P/P_1 exceeds

$$\eta_{cc}=\eta_c+\frac{(ka_0b_0)^2}{4\eta_c}\left(\frac{1}{R_b}-\frac{1}{R_a}\right)^2. \tag{7}$$

For $P=\eta_{cc}P_1$, the self-focus occurs at $z=z_0$, where

$$-(a_0^2+b_0^2)/z_0=a_0^2/R_a+b_0^2/R_b. \tag{8}$$

For higher powers the self-focus will be found at

$$z_f=\frac{z_0}{1+(z_0/ka_0b_0)[(\eta-\eta_{cc})/\eta_c]^{1/2}}. \tag{9}$$

For the fourth entry in Table I, the beam parameters are $a_0=0.179$ mm, $b_0=0.232$ mm, $R_a=4.05$ cm, and $R_b=7.04$ cm. The measured power threshold for the onset of bulk damage was from five to twelve times higher than that for circular beams of comparable dimensions, and the damage first appeared at $z=5.8$ cm from the entrance face. Assuming that the damage should first appear when a catastrophic self-focus forms at $P=\eta_{cc}P_1$, we expect from Eqs. (7) and (8) that the threshold power should be increased by $\eta_{cc}=12.7$ and that the damage at threshold should appear at $z_0=5.51$ cm. The latter figure agrees well with the measured value, and the change in critical power is certainly of the right order. Unfortunately, our knowledge of the influence of the transient electrostrictive contribution to ϵ_2 is too poor to allow us to know which of the first three entries in Table I we should choose as P_1. The first entry ($P_1=0.51$ MW) gives excellent agreement with theory, but the electrostrictive response for an elliptical beam can hardly be as large as that for a circular beam whose diameter equals the small radius of the ellipse. Nevertheless, the agreement with theory is sufficiently good to allow us to conclude that the damage morphology and threshold are well understood in terms of the self-focusing theory.

The theory outlined above gives simple formulas for the powers and distances at which the quantity a^2+b^2 vanishes, but the intensity can become infinite only if the area πab of the beam vanishes. A closer examination of the solutions of Eqs. (1) and (2) shows that a and b both vanish at the same point. Prior to this point, the ratio a/b approaches unity. This is consistent with the observation that the cross sections of the damaged region have a circular shape along the entire length of the damage track. We remind the reader that at some point

between the astigmatic line foci the low-intensity-beam cross section must be circular, but elsewhere it is elliptical

These results imply that difficulties which arise from bulk damage due to self-focusing in high-power optical systems can be avoided or ameliorated by the proper choice of beam parameters.

The authors are grateful to V. Evtuhov for helpful discussions and for providing English translations of Refs. 2 and 3.

*Work supported in part by the Advanced Research Projects Agency under ARPA Order No. 1434 with Air Force Cambridge Research Laboratories.

[1]C. Giuliano and J. Marburger, Phys. Rev. Letters 27, 905 (1971).
[2]V.V. Vorob'yev, Izv. Vysshikh Uchebn. Zavedenii Radiofiz. 13, 1905 (1970).
[3]A.B. Shvartsburg in Ref. 2, p. 1775.
[4]C.R. Giuliano and L.D. Hess in *Damage in Laser Materials*, Nat. Bur. Std. Special Publication No. 341, edited by A.J. Glass and A.H. Guenther (U.S. GPO, Washington, D.C., 1970), p. 76.
[5]W.G. Wagner, H.A. Haus, and J. Marburger, Phys. Rev. 175, 256 (1968).
[6]E. Dawes and J. Marburger, Phys. Rev. 179, 862 (1969). This paper contains a detailed comparison of results of the paraxial-ray—constant-shape approximation with exact numerical solutions.

Observation of the inverse Lamb dip for infrared-microwave two-photon transitions

S.M. Freund* and T. Oka
Division of Physics, National Research Council of Canada, Ottawa, Ontario, Canada
(Received 14 April 1972)

An inverse Lamb dip has been observed for infrared-microwave two-photon transitions in $^{14}NH_3$ and $^{15}NH_3$. The signal was sufficiently strong to be observed on an oscilloscope with a detector time constant of 3 msec. The observations establish a method of measuring differences between laser frequencies and molecular absorption frequencies with high accuracy even if this absorption is outside of the tuning range of the laser lines. A double resonance experiment involving the two-photon inverse Lamb dip has also been conducted.

Most of the observations of an inverse Lamb dip in the infrared and optical regions of spectra have been limited to absorption lines which lie within the tuning range of a laser line.[1] When the absorption line is outside of this range, an electric[2] or magnetic[3] field has been used to tune the spectral lines into resonance. More recently, the inverse Lamb dip has been observed by using pulsed tunable lasers.[4,5] In this letter we report the observation of the inverse Lamb dip for infrared-microwave two-photon transitions. The advantage of this method is that we can measure the frequency of a Lamb dip outside the tuning range of the laser directly and accurately by measuring the microwave frequency.

Since the initial observation of infrared-microwave two-photon transitions,[6] the technique has been used to obtain high-resolution infrared spectra of $^{14}NH_3$ and $^{15}NH_3$.[7] In the experiment, microwave radiation having a tunable frequency is "added" to infrared laser radiation of fixed frequency by using the nonlinearity of a molecular transition process; in effect, we render the laser tunable about the original laser frequency.

An inverse Lamb dip in the absorption is observed when the transition moment of the two-photon transition,

$$(\mu E)_{if} = \langle i | \boldsymbol{\mu}_p \cdot \mathbf{E}_m | m \rangle \langle m | \boldsymbol{\mu}_v \cdot \mathbf{E}_l | f \rangle / 2h\Delta\nu, \qquad (1)$$

is on the order of, or greater than, the pressure-broadening $\Delta\nu_P P$. In Eq. (1) $\mathbf{E}_m$ and $\mathbf{E}_l$ represent the electric field of the microwave and the laser radiation, respectively, which are parallel in this experiment, and $\boldsymbol{\mu}_p$ and $\boldsymbol{\mu}_v$ are the permanent dipole moment (1.467D)[8] and the vibrational transition dipole moment (0.24D),[9] respectively. The letters i, m, and f represent the initial, intermediate, and final molecular states involved in the two-photon transitions, and $\Delta\nu$ is the difference between the frequency of the laser and that of molecular transition (see Fig. 2). With $E_m \simeq 30$ V/cm and $E_l \simeq 100$ V/cm, $(\mu E)_{if}/h$ is on the order of $100/\Delta\nu$ MHz for transitions with high M value (M is the quantum number for the projection of the total angular momentum along the field). Since the pressure-broadening parameter $\Delta\nu_P$ is on the order of 30 MHz/Torr,[8] these electric fields can saturate two-photon transitions with $\Delta\nu \simeq 500$ MHz in ammonia at a pressure, P, of 10 mTorr or lower. The observable $\Delta\nu$ can be increased by simul-

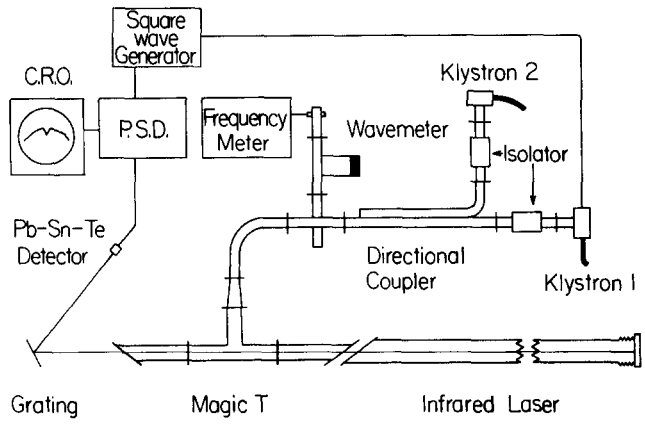

FIG. 1. Block diagram of the apparatus.